Dielectric properties and phase transitions of $[Pb(Zn_{1/3}Nb_{2/3})O_3]_{0.905}(PbTiO_3)_{0.095}$: Influence of pressure

G. A. Samara and E. L. Venturini
Sandia National Laboratories, Albuquerque, New Mexico 87185-1421

V. Hugo Schmidt
Department of Physics, Montana State University, Bozeman, Montana 59717

(Received 17 August 2000; published 18 April 2001)

Studies of the influences of temperature, hydrostatic pressure, dc biasing field, and frequency on the dielectric constant (ε') and loss ($\tan\delta$) of single crystal $[Pb(Zn_{1/3}Nb_{2/3})O_3]_{0.905}(PbTiO_3)_{0.095}$, or PZN-9.5 PT for short, have provided a detailed view of the ferroelectric (FE) response and phase transitions of this technologically important material. While at 1 bar, the crystal exhibits on cooling a cubic-to-tetragonal FE transition followed by a second transition to a rhombohedral phase, pressure induces a FE-to-relaxor crossover, the relaxor phase becoming the ground state at pressures $\geqslant 5$ kbar. Analogy with earlier results suggests that this crossover is a common feature of compositionally disordered soft mode ferroelectrics and can be understood in terms of a decrease in the correlation length among polar domains with increasing pressure. Application of a dc biasing electric field at 1 bar strengthens FE correlations, and can at high pressure restabilize the FE response. The temperature-pressure and temperature-electric field phase diagrams were established. In the absence of dc bias the tetragonal phase vanishes at high pressure, the crystal exhibiting classic relaxor behavior. The dynamics of dipolar motion and the strong deviation from Curie-Weiss behavior of the susceptibility in the high-temperature cubic phase are discussed.

DOI: 10.1103/PhysRevB.63.184104 PACS number(s): 77.22.Gm, 77.80.Bh

I. INTRODUCTION

Complex mixed ABO_3 oxides of the perovskite family find numerous applications in technology because of their exceptional piezoelectric and dielectric properties.[1] Particularly important are compositions near morphotropic phase boundaries (MPB's), where these properties are anomalously high because of the near degeneracy of the two phases which imparts to the lattice greatly enhanced polarizability and ease of poling. In this regard, one of the most widely used materials has been mixed $PbZr_{1-x}Ti_xO_3$ with $x=0.47$ (or PZT 53/47) which is essentially at the MPB for the PZT system.[1] Compositions of the Zr-rich side of this boundary have rhombohedral symmetry at room temperature whereas compositions on the Ti-rich side have tetragonal symmetry. Despite their wide use, PZT's suffer from the fact that they are available only in ceramic form, and thus attainable properties are significantly lower than is potentially achievable with single crystals.

Fortunately, however, it has been found that single crystals of more complex mixed oxides can be relatively easily grown by a flux method over the whole composition range. Specifically, considerable success has been demonstrated in growing mixed crystals between the relaxors $PbMg_{1/3}Nb_{2/3}O_3$ (PMN) or the isomorphous $PbZn_{1/3}Nb_{2/3}O_3$ (PZN) and ferroelectric $PbTiO_3$ (PT).[2,3] Of the two systems, $(1-x)$ PZN-xPT (or PZN-xPT for short) crystals have been attracting a great deal of recent interest because ultrahigh piezoelectric ($d_{33}>2000pC/N$) and electromechanical coupling ($k_{33}\approx 92\%$) coefficients have been achieved for compositions near the MPB ($x\cong 0.09-0.095$).[2,3] These coefficients are much larger than those of PZT 53/47 ceramics and have the potential of greatly advancing transducer/actuator technology.

To better capitalize on these developments, there is a large on-going effort aimed at understanding the physical properties of PZN-xPT's. In earlier work,[4,5] we demonstrated the importance of pressure as a variable in elucidating the physics of ferroelectrics and relaxors, and we have now extended the work to PZN-9.5 at.% PT (henceforth designated PZN-9.5 PT). In particular, we have studied the dielectric properties of this crystal as functions of pressure, temperature, frequency, and electric field and gained much insight into the physics and phase transitions involved.

PZN is a classic relaxor akin to PMN.[2,6,7] It exhibits a broad, frequency-dependent peak in the temperature (T-) dependent static susceptibility or dielectric constant (ε'). The peak ($\sim$410 K) defines a dynamic freezing, or glass-like transition temperature (T_m). As in the case of PMN, symmetry breaking compositional and structural disorder brought about by differences in valence ($5+$ vs $2+$) and ionic radii (0.64 Å vs 0.74 Å) between the Nb^{5+} and Zn^{2+} ions on the B site of the ABO_3 lattice is believed to be responsible for the relaxor character of PZN. The symmetry breaking (rhombohedral) occurs at the nanometer scale leading to the formation of polar nanodomains which exist well above T_m and increase in size on cooling, but never become large enough to precipitate a long-range-ordered FE state at T_m.[6,7] Rather, slowing down of the polarization fluctuations sets in below T_m. Unlike PMN which retains macroscopic cubic symmetry down to cryogenic temperatures, PZN acquires rhombohedral symmetry ($R3m$) at room temperature.[2]

PT, on the other hand, is the classic soft FE mode ferroelectric which transforms on cooling from the cubic

 ©2001 The American Physical Society

paraelectric (PE) phase to a tetragonal ($P4mm$) FE phase at ~760 K.[4] Its addition to PZN, even at the $0.05 \leqslant x \leqslant 0.15$ level, imparts FE character to the mixed crystals.[2] On cooling such crystals transform from the cubic PE phase to a tetragonal FE phase and then to a rhombohedral FE phase.[2]

Following a brief description of the experimental details, the paper presents the main results and their interpretation. A particularly interesting facet of the results is the observation of a pressure-induced ferroelectric (FE)-to-relaxor (R) crossover in the absence of an applied field. A brief account of this crossover phenomenon was presented elsewhere.[8] We have observed a similar crossover in other mixed perovskites[5,9] suggesting that the phenomenon is a general feature of compositionally disordered perovskite ferroelectrics.

II. EXPERIMENTAL DETAILS

The sample used in this study was a thin plate single crystal ($0.22\,\mathrm{cm}^2 \times 0.05\,\mathrm{cm}$) oriented with the pseudocubic (100) axis perpendicular to the large faces.[10] Chrome-gold electrodes were deposited on these faces. The dielectric function, consisting of both the real part (the dielectric constant ε') and the imaginary part (the dielectric loss $\tan\delta$), was studied as function of temperature (77–650 K), hydrostatic pressure (0–15 kbar), frequency (10^2–10^6 Hz) and applied dc biasing field (0–4 kV/cm). Although the apparatus limited the applied bias to 4 kV/cm, it will be shown that fields up to this value produce very meaningful effects that are important for understanding the physics. Pressure was generated using conventional high pressure apparatus using either a 50/50 mixture of normal and isopentanes or helium gas as the pressure transmitting media.[5]

In this study the crystal was exposed to a wide variety of thermal, pressure and biasing field histories. Because sample history has a strong influence on the dielectric response and phase stability of the material, it was necessary to keep track of and specify this history for every set of measurements. For this purpose, we shall use the somewhat common designations field heating or heated (FH), field cooling or cooled (FC), zero field heating or heated (ZFH), zero field cooling or cooled (ZFC), as well as combinations of these and other modifiers throughout the paper.

III. RESULTS AND DISCUSSIONS

A. The 1 bar dielectric response and phase transitions

Kuwata *et al.*[2] reported the temperature-composition phase diagram for the PZN-xPT system for $0 < x < 0.15$. For compositions in the range $0.05 \leqslant x \leqslant 0.12$, samples exhibit on cooling a transition from the high temperature cubic paraelectric (PE) phase to a tetragonal ($P4mm$) FE phase which on further cooling transforms to a rhombohedral ($R3m$) FE phase. Both transitions are thermodynamically first order with substantial thermal hysteresis and somewhat diffuse character. More recently, Tu *et al.*[11a] reported the dielectric properties of a crystal with the same composition ($x = 0.095$) as ours and grown using the same high-temperature flux solution method. They observe a sharp FE transition near 460 K and a diffuse transition near 340 K. The temperatures for both transitions are in agreement with Kuwata *et al.*'s phase diagram.

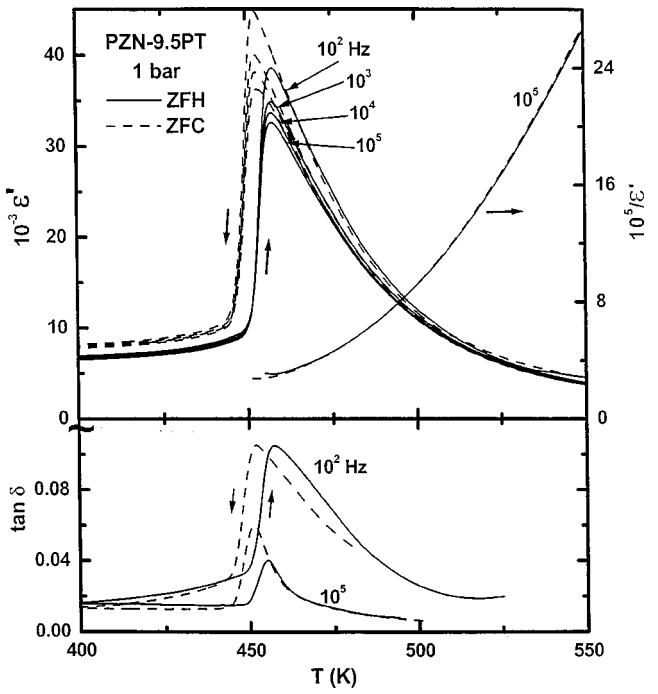

FIG. 1. Temperature dependences of the dielectric constant (ε') and dielectric loss ($\tan\delta$) of PZN-9.5 PT at 1 bar. Results for both zero field heating (ZFH) and zero field cooling (ZFC) are shown. Also shown is the deviation from Curie-Weiss behavior of $\varepsilon'(T)$ in the high-temperature phase.

Figure 1 shows that the dielectric response of our crystal in the unpoled, thermally annealed state is a characteristic FE response. Scans of $\varepsilon'(T)$ and $\tan\delta(T)$ for ZFH and ZFC are shown across the tetragonal-cubic FE transition. The value of the transition temperature ($T_c = 460$ K on heating), the sharpness of the transition, and the 5 K thermal hysteresis agree with earlier observations.[2,11(a)] The relatively weak frequency dispersion in $\varepsilon'(T)$ at and above the peak is characteristic of many mixed ferroelectrics.

On the first ZFH cycle of our sample, the signature of the rhombohedral-tetragonal transition was a weak shoulder in $\varepsilon'(T)$ at ~340 K. The $\tan\delta(T)$ signature was a relatively large decrease in $\tan\delta(T)$ with increasing T followed by a leveling-off above ~340 K. We have investigated this transition in more detail than has been reported heretofore and find that it exhibits complex and subtle behavior that is strongly dependent on the sample history, especially as it pertains to temperature, pressure and biasing field cycling. We shall describe the behavior in Sec. III C.

B. Influence of pressure on the high-temperature dielectric response—the ferroelectric-to-relaxor crossover

Modest pressure has a strong influence on the dielectric response and phase transitions of PZN-9.5 PT. Specifically, pressure shifts T_c to lower temperature and induces a FE-to-R crossover in the dielectric response. The crossover

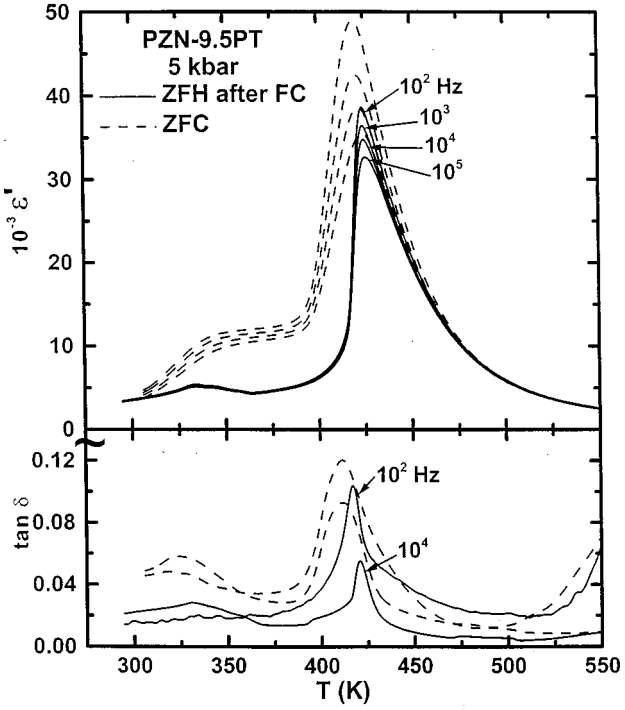

FIG. 2. Temperature dependence of ε' and (tan δ) and of PZN-9.5 PT at 5 kbar on ZFH after FC at 4 kV/cm followed by ZFC.

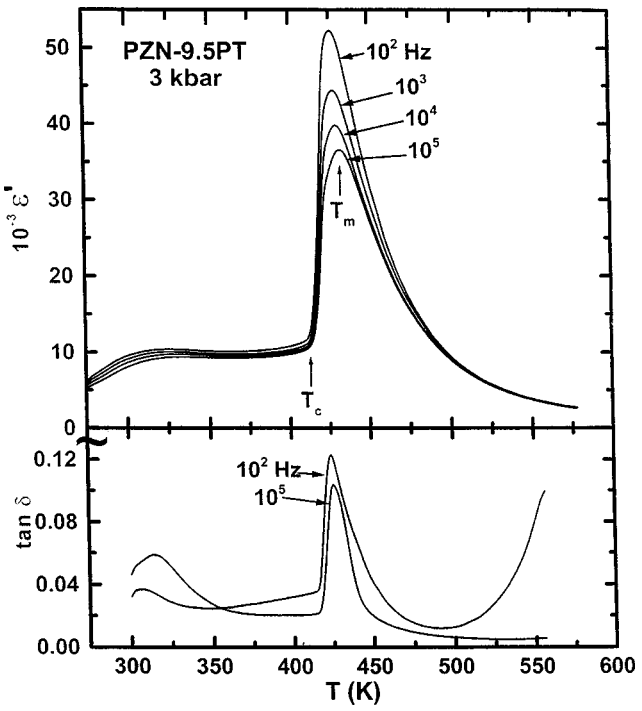

FIG. 3. Temperature dependences of ε' and tan δ of PZN-9.5 PT on ZFC at 3 kbar.

evolves with pressure, but appears to be well-established by ~5 kbar in the absence of a biasing field. Modest fields can, however, restabilize the FE phase (see Sec. III. D). Figure 2 shows some results at 5 kbar. Prior to this experiment the sample was field cooled at 4 kV/cm from 420 to 77 K and then field heated at the same field to 300 K after which the field was removed. This combination of FC/FH stabilized the FE phase as is clearly, shown by the ZFH scan in Fig. 2 which is a characteristic FE response. Subsequent ZFC from 550 K reveals the full relaxor character of $\epsilon'(T)$ as shown. The ZFC scan also shows the $\varepsilon'(T)$ shoulder associated with the low-temperature tetragonal (tet)-rhombohedral (rh) transition.

To further narrow the pressure where the FE-to-*R* crossover occurs, Fig. 3 shows ZFC results at 3 kbar. Whereas at this pressure the sample still exhibits FE character on ZFH, on ZFC it already exhibits mixed character. As can be seen from the figure, on ZFC the sample first enters a relaxor phase at T_m, which subsequently spontaneously transforms to a FE state at T_c. These results suggest that at 3 kbar the FE state is still the ground state of PZN-9.5 PT in zero biasing field. By 5 kbar the *R* state becomes the ground state.

Results at 10 kbar for the sample in the thermally depoled state reveal the full relaxor character of the response.[8] By 15 kbar (Fig. 4) the tet-rh transition is not seen on either ZFH or ZFC, i.e., the tetragonal phase has vanished by this pressure (see Sec. III E). In Fig. 4 the full relaxor character of the response is seen not only in $\varepsilon'(T)$ but also in tan $\delta(T)$.

As already noted, we have now observed this pressure-induced FE-to-*R* crossover in many compositionally disordered ABO_3 oxides and believe it to be a general phenomenon in soft phonon mode systems.[5,8,9] The crossover can be explained (see, e.g., Ref. 5) in terms of a large decrease in the correlation length r_c among polar nanodomains with pressure. Physically, we envision each disorder-related dipole inducing polarization (or dipoles) in adjoining unit cells of the highly polarizable host and forming a dynamic ''po-

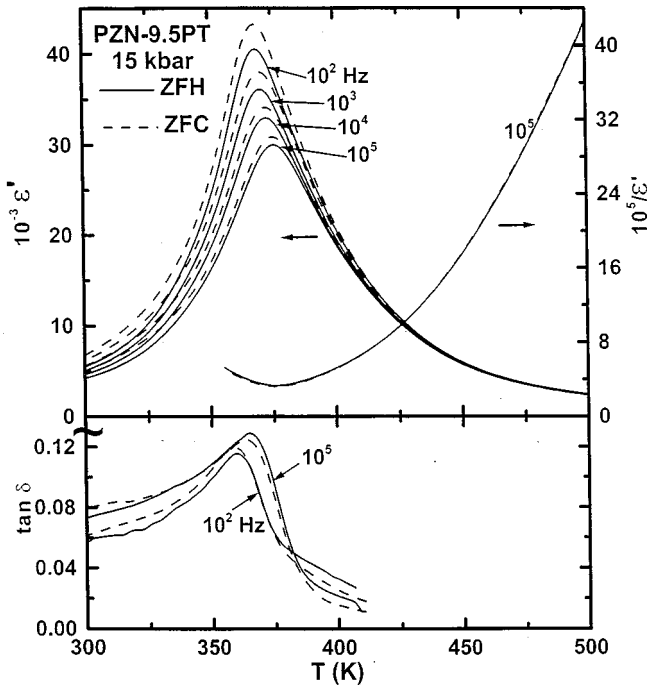

FIG. 4. Temperature dependences of ε' and tan δ of PZN-9.5 PT at 15 kbar for both ZFH and ZFC showing the full relaxor character of the response.

larization cloud'' whose extent is determined by r_c. At high temperature r_c is small, and the polarization clouds are effectively polar nanodomains. With decreasing T at low pressures, the rapidly increasing r_c couples these nanodomains into rapidly growing polar clusters and increases their Coulombic interactions. Ultimately, these clusters percolate (or permeate) the whole sample and precipitate a static, cooperative long-range ordered FE state at $T<T_c$. At sufficiently high pressure, on the other hand, the clusters increase in size on decreasing T in the PE phase, but do not become large enough to permeate the whole sample (or grains) to precipitate a FE transition. Rather, the clusters exhibit dynamic ''slowing down'' of their fluctuations at $T<T_m$ leading to the observed relaxor behavior. Because r_c decreases continuously with increasing pressure, the polar clusters become smaller with increasing pressure. It is thus seen that the FE-to-R crossover results simply from the large decrease in r_c with pressure.

Support for the existence of polar nanodomains in PZN-PT at $T \gg T_c$ is evidenced by deviation from Curie-Weiss behavior of $\varepsilon'(T)$ and a large electrostrictive contribution to the thermal expansion as discussed in Sec. III F. Support also comes from a very recent neutron inelastic scattering study of the soft TO phonon branch of a PZN crystal with 8.0% PT.[11(b)] Results in the cubic phase at 500 K ($\gg T_c$) reveal anomalous behavior in which the TO branch appears to drop precipitously into the transverse acoustic branch at a finite value of the momentum transfer $q = 0.2\,\text{Å}^{-1}$ measured from zone center. This behavior is tentatively attributed to the presence of nanometer sized polar domains in the crystal, and their size is estimated to be 3 nm. These domains can be expected to effectively inhibit the propagation of long wavelength phonons, hence the precipitous drop of the TO branch on approaching zone center.

C. The lower-temperature dielectric response and phase transition

We find that the dielectric response associated with the tet to rh transition is strongly dependent on sample history, especially in the absence of a biasing electric field. We also note that PZN-9.5 PT is essentially at the MPB of this material system. This fact along with the unavoidable compositional fluctuations suggest that both the tet and rh phases should coexist in our sample below T_c at 1 bar. Indeed, polarized light microscopy[12(a)] and neutron diffraction[12(b)] results on a PZN-9 PT crystal clearly show the coexistence of both tetragonal and trigonal (rh) domains at room temperature.

Figure 5 shows the $\varepsilon'(T)$ response of the sample on ZFH at 1 bar following ZFC also at 1 bar. Prior to ZFC, the sample was annealed at 550 K and then ZFC to room temperature. The rh-tet transition is evidenced by the $\varepsilon'(T)$ shoulder at ~340 K and also by a decrease in $\tan\delta(T)$ with increasing T. Because of the coexistence of both phases in the crystal, the transition is not very sharp, and the magnitudes of ε' and $\tan\delta$ varied from run to run depending on how far heating and cooling excursions went beyond the transition. The results at 1 bar also revealed (not shown)

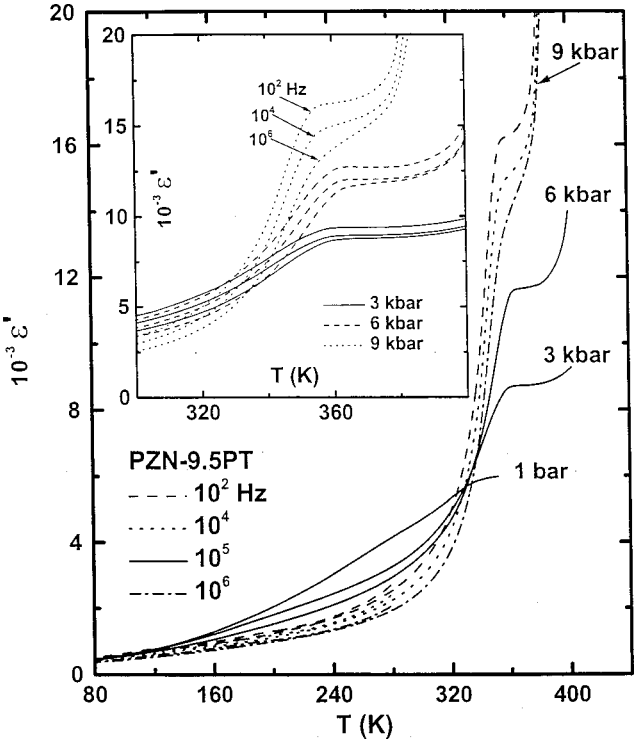

FIG. 5. Temperature dependence of ε' of PZN-9.5 PT at different pressures showing the low-temperature response and the anomaly at the rhombohedral (rh) tetragonal (tet) phase transition. The frequency dispersion in the 9-kbar data is characteristic of the response at other pressures. The inset shows an expanded view of the behavior near the rh-tet transition.

strong frequency dispersion in $\varepsilon'(T)$ reflecting the relaxor response of the sample below T_c as a consequence of the compositional disorder and coexistence of two types of nanodomains.

Next the pressure was raised to 3 kbar at 300 K and the sample ZFC to 77 K. Figure 5 shows the subsequent ZFH response. It is seen that pressure enhances the sharpness of the transition and increases the magnitude of ε' in the tet phase. This trend continues at 6 and 9 kbar as shown. For each pressure, the pressure was raised at 300 K, the sample ZFC to 77 K, and subsequently data taken on ZFH.

Following the 9-kbar run, the temperature was lowered to 285 K and then the pressure was lowered to 1 bar. At these conditions ε' at 10^6 was 2000 which is much smaller than the original 1 bar value of 4900 but about equal to the value of ε' at 9 kbar and 285 K (Fig. 5). In addition to this pressure memory effect, the results in Fig. 5 clearly show that pressure sharpens the distinction between the rh and tet phases and favors the rh phase after pressure release.

With the sample now locked in the rh phase at 285 K and 1 bar, ZFH yields the well-defined rh-to-tet transition shown in Fig. 6. Subsequent ZFC from 410 K shows a large hysteresis in the transition temperature. Stopping at 285 K, ZFH retraced the upper branch up to 410 K. Next, ZFC to 77 K followed the upper branch. Subsequent ZFH from 77 to 400 K followed by ZFC from 400 to 77 K followed the upper branch with little hysteresis and with values of $\varepsilon'(T)$ com-

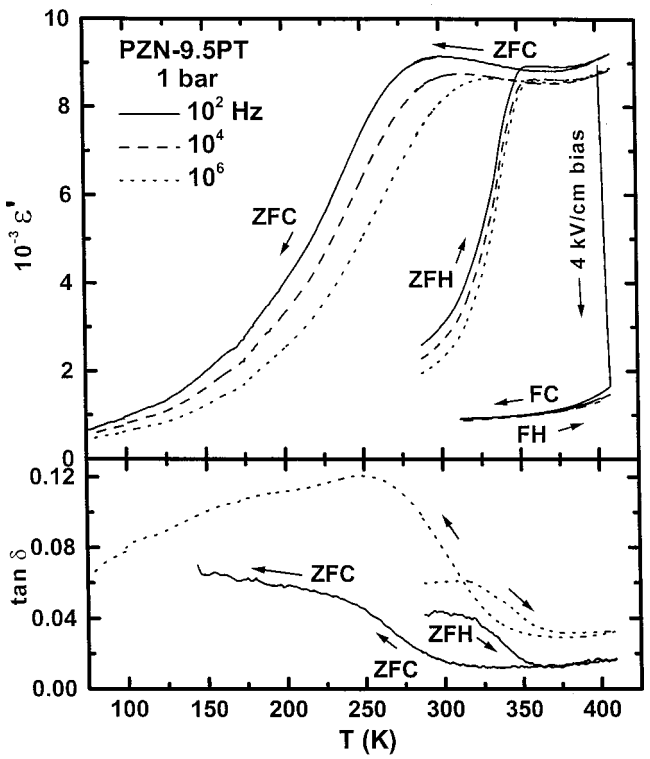

FIG. 6. Temperature dependences of ε' and tan δ of PZN-9.5 PT at 1 bar showing a large hysteretic effect near the rh-tet phase transition. Also shown is the influence of dc bias in the tet phase.

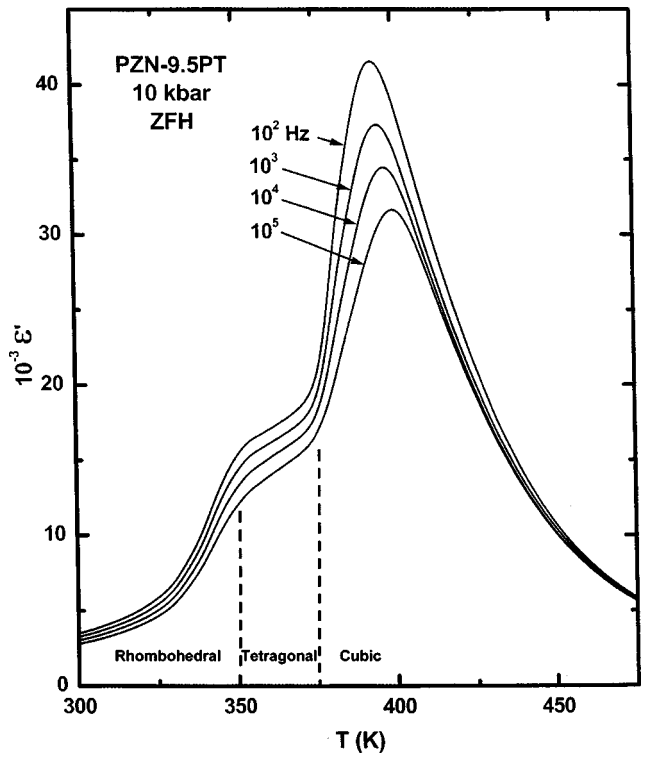

FIG. 7. Temperature dependence of ε' of PZN-9.5 PT at 9 kbar showing the approaching vanishing of the tet phase at higher pressures.

parable to the initial (i.e., before pressurization) 1 bar values in Fig. 5. These results suggest that temperature cycling at 1 bar after recovery from high pressure reverts the sample to a mixture of rh and tet phases. The relatively large values of ε' below 340 K are consistent with this view.

The inset in Fig. 5 suggests that the temperature range of stability of the tet phase decreases markedly with pressure. This is illustrated more clearly by the 9-kbar response in Fig. 7 which shows that the tet phase is stable over <30 K temperature range at this pressure compared to >120 K range at 1 bar. As we noted earlier, this phase vanishes completely above 10 kbar (see, e.g., Fig. 4 and Sec. III E).

D. The influence of dc biasing electric fields

The application of a dc biasing field can provide much insight into the energetics and kinetics of domain reorientation as well as the growth of polar domains in relaxor ferroelectrics. Cooling relaxors in the presence of a field (FC) aligns the polar nanodomains and increases their correlations and size, effectively cancelling the influence of random fields. For sufficiently large fields the domains become large (microns in size) and lead to the onset' of long-range order and normal ferroelectricity. This is a field-induced nano-to-macro domain transition. Evidence for such a transition in relaxors can be easily inferred from the dielectric response and can often be seen in TEM images.

As noted above, the relaxor phase becomes the ground state of PZN-9.5 PT at pressures $\geqslant 5$ kbar; however, we find that dc biasing fields in the 2–4 kV/cm range are sufficient to restabilize normal FE response at high pressures. To study these field effects, the sample was pressure annealed at 5 kbar and 300 K for 2 days subsequent to ZFC and ZFH runs at 15 kbar. As noted in Sec. III C, pressure favors the rh phase, ''locks in'' the rh domain structure, and sharpens the signature of the rh-tet transition. This is clearly seen in Fig. 8. The initial ZFH scan from the starting condition of the sample shows a relatively sharp rh-to-tet transition, a significantly higher transition temperature, and a larger ε' in the tet phase (compare Figs. 5 and 8). These results make it clear that pressure history has a substantial influence on the rh-tet transition. Also noteworthy on the ZFH scan in Fig. 8 is the sharp FE transition at $T_c \simeq 410$ K. However, on further heating the sample quickly enters the relaxor phase consistent with our conclusion in Sec. III B that this phase is the ground state of the sample at 5 kbar in the absence of biasing field.

Next a 4 kV/cm bias was applied at 520 K and 5 kbar, i.e., in the cubic phase. The subsequent FC trace in Fig. 8 shows that under bias the sample exhibits a diffuse FE transition at $T_c = 443$ K. Although there is some frequency dispersion in the magnitude of ε' at T_c, there is no dispersion in T_c, as in normal ferroelectrics. We also note that T_c at 4 kV/cm is much higher than T_m or T_c under ZF conditions. We shall come back to this point in Sec. III E. Also noteworthy in Fig. 8 is the much lower value of ε' in the tet phase under bias. This effect is a consequence of the ability of the field applied in the $\langle 001 \rangle$ direction to align and clamp the polar domains in the tetragonal phase, thereby reducing the polarizability of the lattice, and thus ε'. It is a common feature of anisotropic

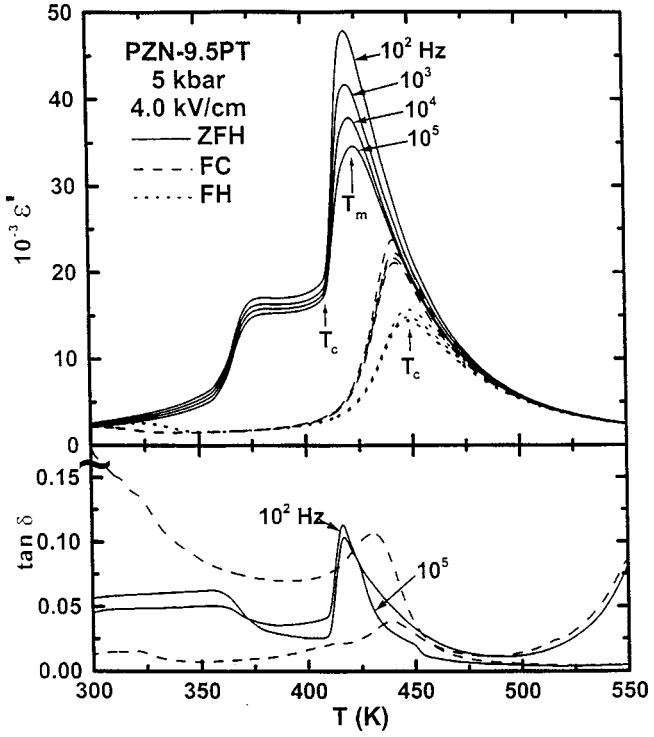

FIG. 8. Temperature dependences of ε' and tan δ of PZN-9.5 PT at 5 kbar showing the influence of dc bias.

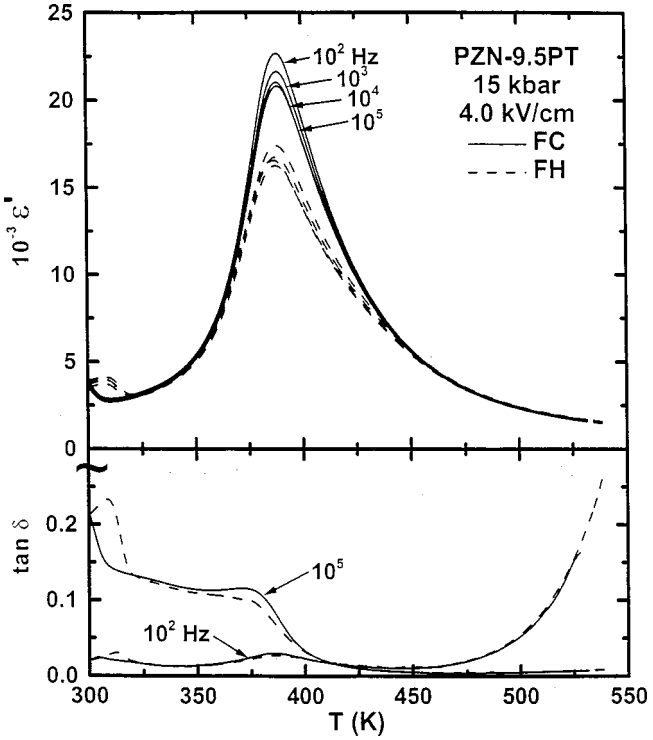

FIG. 9. Temperature dependences of ε' and tan δ of PZN-9.5 PT at 15 kbar under dc bias.

tetragonal FE crystals such as $BaTiO_3$ and $KNbO_3$ whereby a field in the $\langle 001 \rangle$ direction makes ε_3' much smaller than ε_1'.

After FC the sample to 295 K, it was FH under the same conditions (i.e., 4 kV/cm and 5 kbar). The dielectric response is also shown in Fig. 8. Here we see evidence for the rh-to-tet transition below 350 K and a diffuse FE transition at $T_c = 448$ K. Again there is no dispersion in T_c, but there is a distinct thermal hysteresis in T_c between FH and FC indicating the first-order character of this diffuse phase transition. This feature is qualitatively different from the behavior of the relaxor phase where there is no thermal hysteresis in T_m—a fact that emphasizes the FE character of the transition under bias. Also notable in Fig. 8 is the larger amplitude of ε' near T_c on FC compared to FH. This is a consequence of the first-order character of the transition. Additionally, the peak values of ε' of the relaxor phase are larger than for the FE phase as shown and consistent with T_m being lower than T_c.

The above sequence of experiments was repeated at 10 kbar and then at 15 kbar. The responses at the two pressures were qualitatively similar, namely, the 4 kV/cm bias reestablishes the FE character of the transition at 10 kbar and marginally so at 15 kb. Results on FC from 530 to 300 K followed by FH from 300 to 540 K at 15 kbar are shown in Fig. 9. There is a slight hint of frequency dispersion, but practically no thermal hysteresis in T_c at this pressure. T_c is considerably higher than T_m in the absence of a field at the same pressure (compare Figs. 4 and 9), and the character of the transition is different for the two cases. Although the field has clearly restabilized the FE phase, nevertheless there is a hint in the $\varepsilon'(T)$ data in Fig. 9 that the sample exhibits weak relaxor character under these conditions. This feature is evidenced more clearly in the tan $\delta(T)$ signature of the transition which exhibits larger values of tanδ below T_c than is associated with a normal FE transition. These data suggest that 4 kV/cm is just barely sufficient to reinforce the FE character of PZN-9.5 PT at 15 kbar. This is as expected: the higher the pressure, and therefore the stronger the relaxor character, the higher is the biasing field needed to restabilize the FE phase. Also noteworthy in Fig. 9 is the reemergence of the rh-tet transition below 325 K under bias. Recall that this transition vanishes by 15 kbar in the absence of bias (see Fig. 4 and Sec. III E).

There is a feature in the results that should be noted here, namely the influence of the dc bias on the dielectric signature of the rh-tet transition. Reference to Fig. 5 shows that in the absence of bias, the signature of the transition is a shoulder in $\varepsilon'(T)$, ε' in the tet phase being larger than in the rh phase. In the presence of a field, however, the picture is reversed and there is a dip in $\varepsilon'(T)$ in going from the rh to the tet phase as can be seen in Figs. 8 and 9. This field effect is due to the aforementioned $\langle 001 \rangle$ field alignment and clamping of the polar domains in the tet phase which strongly reduces ε'. The large magnitude of the effect is clearly seen in the inset in Fig. 6. Prior to this experiment the sample had not been exposed to bias, but underwent a couple of ZFC and ZFH cycles between 77 and 410 K at 1 bar after pressure cycling to 9 kbar. In the inset, the sample, nominally in the tet phase but in reality a mixture of tet and rhombohedral domains (upper branch), was first ZFH from 290 to 405 K. The $\varepsilon'(T)$ response including frequency dispersion is comparable to that in Fig. 6. A 4 kV/cm bias was

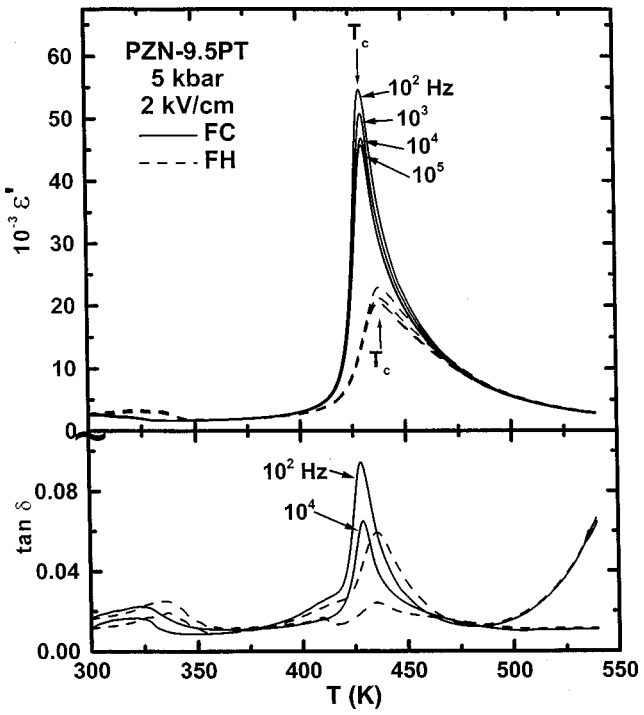

FIG. 10. Temperature dependences of ε' and tan δ of PZN-9.5 PT at 5 kbar under dc bias.

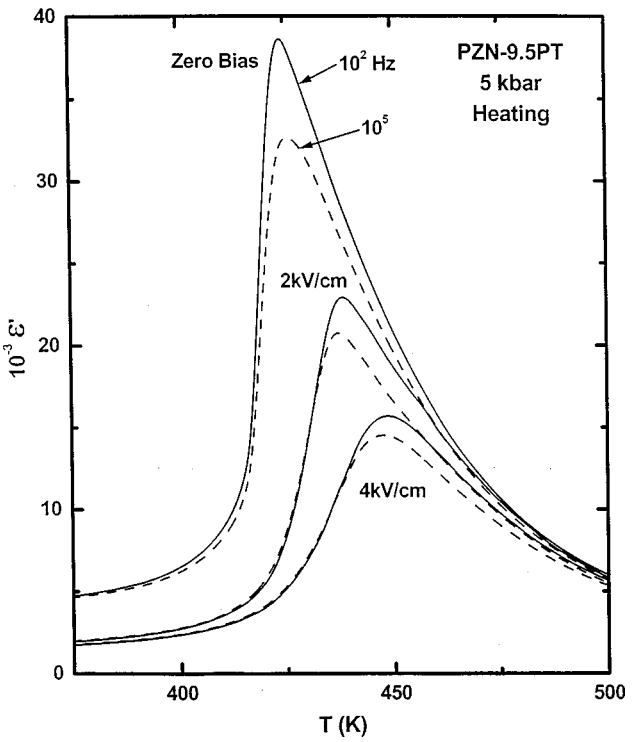

FIG. 11. The influence of dc bias on the dielectric response of PZN-9.5 PT at 5 kbar.

then applied at 405 K resulting in the large suppression of ε' and reduction of the dispersion shown which are associated with field stabilization of the tet FE phase and clamping of its domain. We repeated this experiment at 6 kbar and 4 kV/cm bias and found qualitatively similar results.

In the next series of experiments the pressure was lowered from 15 to 5 kbar under 4 kV/cm bias at 540 K, i.e., in the high-temperature cubic phase. The bias was then lowered to 2 kV/cm at 540 K. Figure 10 shows the subsequent FC followed by FH responses. Clearly again the bias stabilizes the FE phase. There is no frequency dispersion in T_c, but there is significant (7 K) thermal hysteresis pointing to the first-order character of the transition. The FE character of the transition is also seen in the tan $\delta(T)$ data in Fig. 10 where tan δ drops to low values below the peak at T_c.

At 10 kbar, the 2 kV/cm bias is marginally capable of reestablishing the FE character of the transition. The $\varepsilon'(T)$ and tan $\delta(T)$ responses gave indications of some weak relaxor character at this pressure.

Figure 11 summarizes the influence of dc bias on the $\varepsilon'(T)$ response on heating at 5 kbar. Most notable are the shift of the transition to higher temperatures (see Sec. III E) and the large reduction in ε' at the transition with increasing field. Both effects are associated with the alignment of polar domains with the field which implies (i) the need for more thermal energy to disrupt this alignment (thus a higher T_c) and (ii) lower lattice polarizability (thus lower ε') as was pointed out above.

E. Temperature-pressure and temperature-electric field phase diagram

Figure 12 shows the temperature-pressure phase diagram of PZN-9.5 PT at zero bias. For the cubic-tet phase boundary we show data on heating only. The relatively small thermal hysteresis in the Curie temperature T_c was mentioned in Sec. III B. At 1 bar $T_c = 460$ K and decreases with pressure at a rate $dT_c/dP = -6.6 \pm 0.3$ K/kbar. This slope is comparable to that observed for many pervoskite ferroelectrics and is well understood in terms of soft mode theory.[4] Although to our knowledge no well-defined FE (i.e., TO) soft mode has been observed for this crystal, the very large ε' and its Curie-like temperature dependence in the cubic phase are clearly indicative of soft TO-like excitations in the lattice. Additionally, it should be noted that compositional fluctuations in mixed crystals broaden the phonon spectrum and make it difficult to observe distinct modes. The first-order nature of the FE transition in PZN-9.5 PT also implies that the frequency of the soft mode remains finite at T_c.

As was pointed out in Sec. III B, PZN-9.5 PT exhibits a FE-to-R crossover in the 3–5 kbar range. Figure 12 shows the cubic paraelectric-to-tet relaxor phase boundary for 10^2 and 10^5 Hz on heating, where $T_m(P)$ is linear up to 15 kbar. The slopes, $dT_m/dP = -5.2 \pm 0.4$ K/kbar at 10^2 Hz and -4.9 ± 0.4 K/kbar at 10^5 Hz, are distinctly lower than for T_c/dP, a feature that we have observed earlier in other materials.[5]

The tet-rh phase boundary is, as already discussed in Sec. III C, very dependent on sample history in zero bias, and it is thus difficult to define a distinct boundary. In Fig. 12 we plot all of our data points obtained in zero bias on both heating and cooling. Given near each data point is the order of the run. Between any two runs the sample may have been exposed to a variety of pressure, temperature or field cycles as described in Sec. III C. The dashed line drawn through the

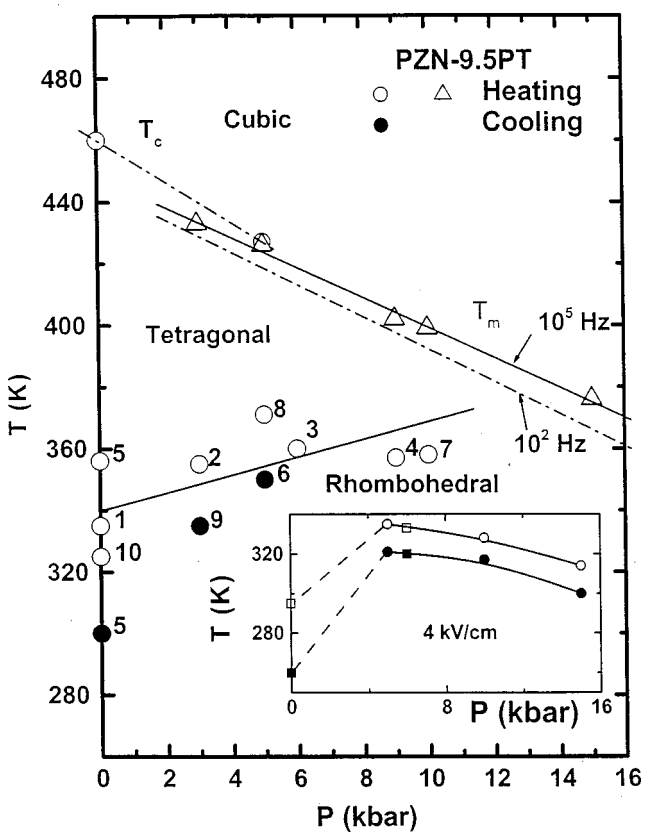

FIG. 12. Temperature-pressure phase diagram of PZN-9.5 PT in the absence of bias. The numbers next to the data points at the tetragonal-rhombohedral phase boundary refer to the order in which the data were obtained. The inset shows the rh-tet phase boundary under bias.

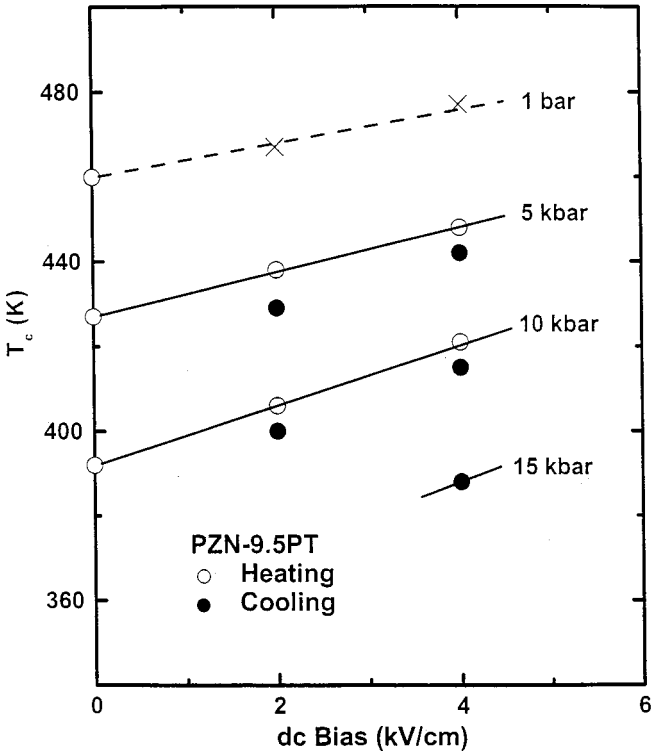

FIG. 13. Influence of dc bias and pressure on the cubic-tetragonal FE transition temperature of PZN-9.5 PT.

data in Fig. 12 is a rough guide to the eye. What can be said with some certainty is that the transition temperature increases with pressure (at least initially), there is a relatively large thermal hysteresis, and the tet phase completely vanishes, certainly by 15 kbar or possibly sooner as described in Sec. III B. In this study we did not explore the region where the phase boundaries meet.

The large scatter in tet-rh transition temperatures is undoubtedly related to the fact that PZN-9.5 PT is very near the MPB for this material system, and the sample in zero field consists of a fluctuating mixture of tet and rh domains, the preponderance of each of which depends on sample history. The application of bias sharpens the distinction between the two phases, reduces the scatter in transition temperatures and reverses the slope of the phase boundary at high pressure as seen in the inset in Fig. 12.

As described in Sec. III D, bias fields along the pseudocubic ⟨001⟩ direction stabilize the FE character of the cubic-tet transition. Figure 13 shows the field dependence of T_c of this transition. At 1 bar the data points at 2 and 4 kV/cm (denoted by *x*) were deduced from extrapolation of the high pressure data under bias to zero pressure. The slope is $dT_c/dE = 3.8$ (K cm/kV) which is comparable to a value of 3.2 (K cm/kV) obtained by Kuwata *et al.*[2] for PZN-9.0 PT with the bias along the pseudocubic ⟨111⟩ direction. The larger value for our sample is consistent with the sample being closer to the MPB of PZN-xPT. As shown in Fig. 13 dT_c/dE increases to 5.0 (K cm/kV) at 5 kbar and 7.0 (K cm/kV) at 10 kbar. This behavior is also qualitatively as expected: the lower T_c, the softer the lattice, and the stronger is the bias field effect. At 15 kbar the FE phase could be restabilized at 4 kV/cm but not at 2 kV/cm, hence there is only one datum point for this pressure. Clearly pressure and dc bias have opposite effects on T_c.

F. Deviation from Curie-Weiss behavior

It is now well established that whereas $\varepsilon'(T)$ of a normal ferroelectric obeys the Curie-Weiss law, $\varepsilon' = C/(T-T_0)$, above the transition temperature T_c, the $\varepsilon'(T)$ response of relaxors exhibits strong deviation from this law over a broad range of temperatures above T_m.[13] In this expression C is the Curie constant and T_0 is the Curie-Weiss temperature. Figures 1 and 4 illustrate this deviation for PZN-9.5 PT in measurements at two different pressures. These results make it clear that a nearly linear $1/\varepsilon'$ vs T response is obtained only at temperatures $\gg T_m$.

Smolensky and Agranovskaya[15] were the first to note deviations from Curie-Weiss behavior for relaxor ferroelectrics and treated the effect in the context of a model based on compositional inhomogeneity predicting an $\varepsilon' \propto 1/(T-T_0)^2$ behavior. Others have also used the expression

$$\varepsilon' \propto (T-T_0)^{-Y} \tag{1}$$

with $Y=2$ to describe the deviation for different relaxors. Our data on PZN-9.5 PT follow fairly well a $Y=2$ regime

between T_m and ~590 K at 1 bar (Fig. 1) and between T_m and ~450 K at 15 kbar (Fig. 4). More generally, it has been observed[13,14] that no single value of Y is found which uniquely describes the $\varepsilon'(T)$ dependence of relaxors. Rather, different Y's can be found for given relaxors depending on the width of the temperature window above T_m and on the frequency of the measurement.

It is worth noting here that although there is no unambiguous physical justification for Eq. (1) with $Y=2$ for relaxors, a similar result with $Y=2$ is predicted on the basis of lattice dynamical models solved within the framework of quantum statistical mechanics to describe deviation from Curie-Weiss behavior in the quantum displacive limit ($T_c \equiv 0$) of ferroelectrics.[15,16] In this case the deviation is attributed to quantum mechanical fluctuations. Deviations from Curie-Weiss behavior are commonly observed in the temperature dependence of the magnetic suspectibility χ of spin glasses above the freezing temperature of spin fluctuations T_f.[17] For an ideal superparamagnet, i.e., for noninteracting paramagnetic particles or clusters, $\chi(T)$ exhibits Curie-Weiss behavior. This behavior is obtained in spin glasses for temperatures $\gg T_f$. At lower temperatures, deviation from the Curie-Weiss law is attributed to strong local magnetic correlations and the onset of local (spin-glass) order below T_f. Sherrington and Kirkpatrick[18] developed a model which relates $\chi(T)$ below T_f to the local order parameter q. The expression is

$$\chi = \frac{C[1-q(T)]}{T - T_0[1-q(T)]}, \tag{2}$$

where it is seen that q is a function of temperature. Clearly q and its temperature dependence can be evaluated from $\chi(T)$ data and the values of C and T_0 determined from the high temperature $\chi(T)$ response above T_f which follows a Curie-Weiss law. In this high-temperature limit $q \Rightarrow 0$ and Eq. (2) simply reduces to a Curie-Weiss form. Equation (2) can then be thought of as a modified Curie-Weiss law where both C and T_0 are functions of temperature.

If we presume, as we believe to be the case, that the deviation from Curie-Weiss behavior in relaxors is due to correlations among local polar nanodomains, then we can invoke for $\varepsilon'(T)$ an expression similar to that in Eq. (2), where the local order parameter due to correlation between neighboring polar regions of polarizations P_i and P_j is $q \equiv \langle P_i P_j \rangle^{1/2}$. Such an equation has been shown to provide a satisfactory description of the $\varepsilon'(T)$ response of the relaxor PMN,[14] and we find it to be also satisfactory for PZN-9.5 PT.

By extending our $\varepsilon'(T)$ data on PZN-9.5 PT to higher temperatures at 1 bar we have observed a Curie-Weiss response between 590 and 680 K as is clearly shown by the linear $1/\varepsilon'$ vs T behavior in Fig. 14. These data yield $C = 1.67 \times 10^5$ K, a value characteristic of perovskite ferroelectrics, and $T_0 = 525$ K. Similarly, at 15 kbar we find a linear $1/\varepsilon'$ vs T response above 460 K with $C = 1.79 \times 10^5$ K and $T_0 = 425$ K. Assuming the decrease of T_0 with pressure is linear up to 15 kbar, these results yield $dT_0/dP = -6.6$ K/kbar, which is essentially the same slope as for T_c (Sec. III B) as expected. In Fig. 14 deviation from Curie-Weiss behavior sets in below ~590 K. This is the temperature where dipolar correlations lead to the condensation of polar nanodomains which subsequently grow with decreasing temperature (see Sec. III B). That this contention is indeed the case is evident from the thermal expansion and birefringence data of Uesu *et al.*[12(b)] on a sample of PZN-9.0 PT. These results show deviation from the normal thermal expansion and nonvanishing of the birefringence at temperatures extending well above T_c. The inset in Fig. 14 is a replot of the data of Uesu *et al.* on the temperature dependence of the (222) lattice spacing. Lattice spacings for ABO_3 perovskites are found to be essentially linear in the temperature range of the data in the inset. It is seen that deviation from linearity sets in on cooling at ~575 K which is very close to the 590 K where deviation from Curie-Weiss behavior sets in for our PZN-9.5 PT sample (Fig. 14). The difference in the two temperatures is largely due to the fact that our sample contains 0.5 mol % more $PbTiO_3$.

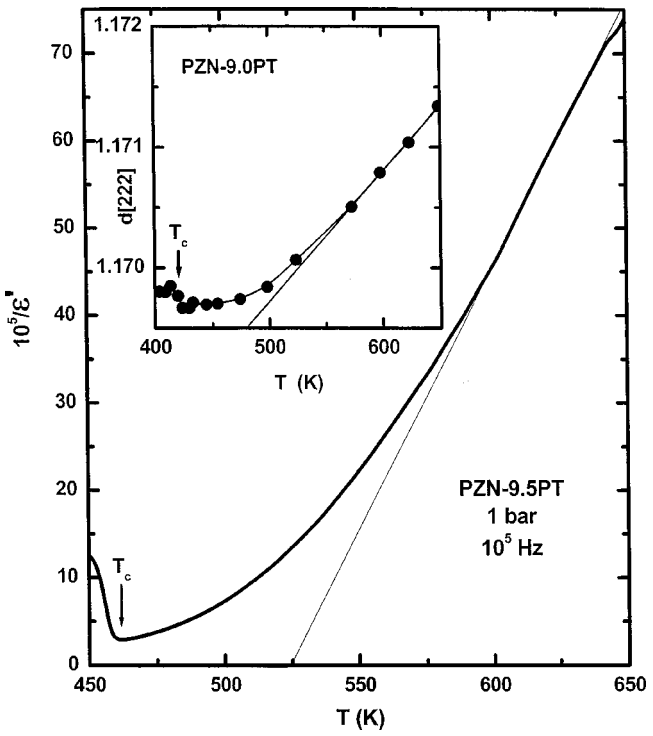

FIG. 14. Temperature dependence of $1/\varepsilon'$ showing that Curie-Weiss behavior obtains above ~590 K. (The glitch above 680 K is believed to be an artifact.) The inset shows the temperature dependence of the (222) lattice spacing for PZN-9.0 PT after Uesu *et al.*[12(b)]

Deviation from normal thermal expansion in relaxors is due to electrostriction. Above T_m in relaxors there are random + and − fluctuations of any vector component of the dipolar polarization (P_d) of nanodomains resulting in zero average polarization, i.e., $V^{-1}\Sigma P_{\mathrm{di}} V_i = 0$. However, there is nonvanishing mean square dipolar polarization, i.e., $V^{-1}\Sigma P_{\mathrm{di}}^2 V_i \neq 0$. Here V is the total volume and $V^{-1}\Sigma V_i$ is the volume fraction occupied by nanodomains—a quantity that increases with decreasing temperature. Thus, the existence of polar domains is manifested in properties which depend on the mean P_d^2. Electrostriction is such a property,

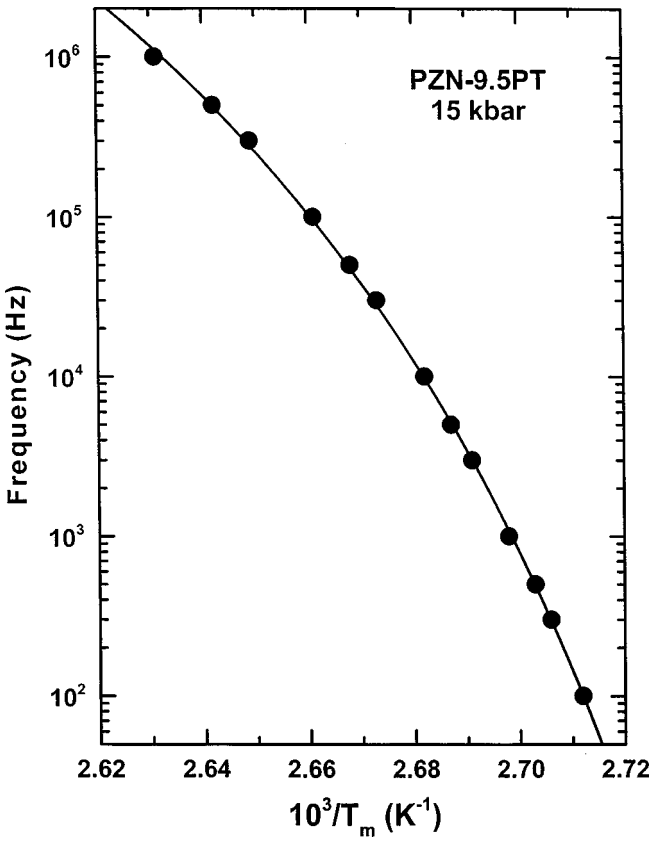

FIG. 15. Temperature dependence of the relaxation frequency of polar nanodomains in PZN-9.5 PT showing the non-Arrhenius response.

as can be seen from the following expression for the total strain (X_{11}) for a cubic perovskite:[20]

$$x_{11}=\alpha(T-T_0^*)+(Q_{11}+2Q_{12})P_d^2. \tag{3}$$

In Eq. (3) the first term on the right is the thermal strain and the second is the electrostrictive strain. α is the linear thermal expansion coefficient, T_0^* is a reference temperature, and Q_{11} and Q_{12} are electrostrictive coefficients. Reference to Eq. (3) clearly shows that the deviation from linearity below ~575 K in the inset in Fig. 14 is due to electrostriction which evolves with decreasing T. It is then also clear that the deviation from Curie-Weiss behavior for our sample below 590 K is due to the formation and correlations among these nanodomains.

G. Dynamics of the polar domain freezing process

As already noted (Sec. III B), the pressure-induced relaxor phase of PZN-9.5 PT evolves continuously with pressure. Results such as those in Fig. 4 provide a detailed view of the dynamics of the polar domain freezing process; they define relaxation frequencies f corresponding to the peak temperature T_m and characteristic relaxation times $\tau=1/\omega$, where $\omega=2\pi f$ is the angular frequency. Although for our sample at 15 kbar T_m increases by only 12 K between 10^2 and 10^6 Hz (a relatively narrow range), the temperature dependence of τ is found to be non-Arrhenius (Fig. 15) as is true for most relaxors.[13,19] The data can be fit by the Vogel-Fulcher equation

$$\tau^{-1}=\omega=\omega_0\exp[-E/k(T_m-T_0)] \tag{4}$$

which is applicable to many relaxational phenomena.[19] Accurate evaluation of the parameters in Eq. (3) requires data over broad ranges of frequencies/temperatures. Nevertheless, fit of our limited 15 kbar data yields values of these parameters that are compatible with those observed for other perovskite relaxors,[5,13] namely, $E=32$ meV, $T_0=353$ K, and $\omega_0=4.2\times10^{12}$ s^{-1}. In our earlier work we have observed that E decreases with pressure, and we expect the same behavior for the present case. The decrease in E is a manifestation of the decrease in the size of the polar domains with pressure (Sec. III B). Simply stated, smaller domains are easier to reorient than larger domains, hence a lower E.

At this point we should note that relaxor behavior is also observed at the tet-rh phase transition at 1 bar and low pressures as is evident in the data in Figs. 5 and 6. We did not attempt to analyze this behavior because of the aforementioned strong dependence on sample history.

IV. SUMMARY AND CONCLUDING REMARKS

The present work has provided much new insight into the physics and phase transitions of PZN-9.5 PT, and we believe that the results are characteristic of other compositions near the morphotropic phase boundary (MPB) of this material system. Specifically, evidence for the existence of polar nanodomains at $T\gg T_c$ is revealed by the observed pressure-induced FE-to-relaxor crossover and by the deviation from Curie-Weiss behavior of $\varepsilon'(T)$. This evidence is supported by recent thermal expansion measurements[12(b)] on PZN-9.0 PT and an inelastic neutron scattering study[11(b)] of the soft TO mode in PZN-8.0 PT. We have observed the pressure-induced crossover in a variety of other mixed, disordered ABO_3 perovskites,[5,9,19] and it thus appears to be a general phenomenon of systems in which polar nanodomains exist in a highly polarizable, or soft FE mode host lattice. The relaxor phase evolves continuously with increasing pressure and becomes the ground state of PZN-9.5 PT above 5 kbar. The temperature-pressure and temperature-electric field phase diagrams of PZN-9.5 PT were determined. At pressures below the FE-to-relaxor crossover, the dielectric results indicated the presence of mixed tetragonal and rhombohedral domains below T_c as can be expected for a composition near the MPB. This mixed phase character made the properties of the crystal very strongly dependent on the electrical and stress history of the sample. Although pressure sharpens the distinction between the tetragonal and rhombohedral phases and favors the latter, the mixed phase character made it difficult to accurately establish the equilibrium pressure-temperature phase boundary for the tetragonal-rhombohedral phase transition. An approximate phase boundary has been determined, and it shows that the tetragonal phase vanishes above 10 kbar. By increasing the sizes and correlations of polar nanodomains, dc biasing fields counter the influence of pressure. In particular, an interesting interplay between pressure and dc bias was demonstrated, and it was shown that a

sufficiently large bias can restabilize the FE phase at a given pressure.

ACKNOWLEDGMENTS

It is a pleasure to acknowledge the excellent technical support of L. V. Hansen. The work at Sandia was supported by the Division of Materials Sciences, Office of Science, U.S. Department of Energy under Contract No. DE-AC04-94AL85000. Sandia is a multiprogram laboratory operated by Sandia Corporation, a Lockheed Martin Company for the U.S. Department of Energy. The work at Montana State was supported by DOD EPSCOR Grant No. N00014-99-1-0523

[1] M. E. Lines and A. M. Glass, *Principles and Applications of Ferroelectric and Related Materials* (Clarendon Press, Oxford, 1977), and references therein.

[2] J. Kuwata, K. Uchino, and S. Nomura, Jpn. J. Appl. Phys. **21**, 1298 (1982), and references therein.

[3] S.-E. Park and T. R. Shrout, J. Appl. Phys. **82**, 1804 (1997), and references therein.

[4] G. A. Samara and P. S. Peercy, in *Solid State Physics*, edited by H. Ehrenreich, F. Seitz, and D. Turnbull (Academic Press, New York, 1981), Vol. 36, p. 1.

[5] G. A. Samara, Phys. Rev. Lett. **77**, 314 (1996); J. Appl. Phys. **84**, 2538 (1998), and references therein.

[6] N. de Mathan, E. Husson, G. Calvarin, J. R. Gavarri, A. W. Hewat, and A. Morell, J. Phys.: Condens. Matter **3**, 8159 (1991), and references therein.

[7] D. Viehland, M. Wuttig, and L. E. Cross, Ferroelectrics **120**, 71 (1991).

[8] G. A. Samara, E. L. Venturini, and V. H. Schmidt, Appl. Phys. Lett. **76**, 1327 (2000).

[9] G. A. Samara and L. A. Boatner, Phys. Rev. B **61**, 1 (2000).

[10] The crystal was flux grown and purchased from TRS Ceramics, 2820 E. College Ave., State College, PA 16801.

[11] (a) C.-S. Tu, F.-C. Chao, C.-H. Yeh, C.-L. Tsai, and V. H. Schmidt, Phys. Rev. B **60**, 6348 (1999); (b) P. M. Gehring, S.-E. Park, and G. Shirane, Phys. Rev. Lett. **88**, 5216 (2000).

[12] (a) Z.-G. Ye, M. Dong, and L. Zhang, Ferroelectrics **229**, 223 (1999); (b) Y. Uesu, Y. Yamada, K. Fujishiro, H. Tazawa, S. Enokido, J. M. Kiat, and B. Dkhil, *ibid.* **217**, 319 (1998).

[13] See, e.g., *Proceedings of the International Seminar on Relaxor Ferroelectrics* [Ferroelectrics **199** (1997)].

[14] D. Viehland, S. J. Jang, L. E. Cross, and M. Wuttig, Phys. Rev. B **46**, 8003 (1992).

[15] G. Smolensky and A. I. Agranovskaya, Sov. Phys. Solid State **1**, 1429 (1959).

[16] G. A. Samara, Physica B **150**, 179 (1988), and references therein.

[17] See, e.g., K. Binder and A. P. Young, Rev. Mod. Phys. **58**, 801 (1987); see also A. Morgownik and J. Mydosh, Phys. Rev. B **24**, 5277 (1981); K. Rao *et al.*, *ibid.* **27**, 3104 (1983).

[18] D. Sherrington and S. Kirkpatrick, Phys. Rev. Lett. **35**, 1792 (1975).

[19] G. A. Samara, Ferroelectrics **117**, 347 (1991), and references therein. These references also discuss the generality and applicability of the Vogel-Fulcher equation.

[20] See, e.g., L. E. Cross, Ferroelectrics **76**, 241 (1987).